CHIMIA 52 (1998) Nr. 10 (Oktober)

Chimia 52 (1998) 585–590
© Neue Schweizerische Chemische Gesellschaft
ISSN 0009–4293

Sulfides, Zeolites, and Nanotowers

Roel Prins*, **Andreas Kogelbauer**, and **Thomas Weber**

Abstract. Three new classes of materials, which we developed and use in our catalytic research, are described. Layered and intercalated sulfides are studied for their use as model compounds for hydrodesulfurization catalysis. Dealuminated zeolites and other mesoporous materials contain mesopores which enhance diffusion and, thus, the effectiveness of zeolitic materials in liquid-phase reactions. Using lithographic techniques, nanotowers are manufactured from layers of metals and insulators placed on silicon wafers. The nanotowers are studied as model catalysts, especially for investigating size effects in heterogeneous catalysis.

Introduction

The improvement of existing catalysts and the invention of new ones goes hand-in-hand with research on catalytic materials. In this contribution, three classes of materials will be described. Layered intercalated molybdenum sulfides are model systems for hydrodesulfurization, the removal of sulfur atoms from sulfur-containing molecules, such as (di)benzothiophene, from oil fractions. Zeolites belong to an industrially very important class of compounds which are used especially as detergents and as catalytic cracking catalysts. Their use in liquid-phase reactions is hampered by the slow diffusion through the narrow micropores. The introduction of mesopores into zeolitic materials and the creation of materials with well-defined mesopores will be introduced.

As well as zeolitic and other acidic catalysts, metal catalysts are another main class of catalysts. They are industrially manufactured using methods which, almost without exception, lead to a broad distribution of particle sizes, and this has hampered progress in understanding the mechanism of the reactions. In particular, the understanding of the so-called structure-sensitive reactions, in which the rate of the reaction is dependent upon the crystallographic surface on which the reaction occurs, has been hindered. This is because small metal particles have different crystal-surface planes (more high-index planes) than particles which are, for the most part, terminated by (111), (100), and (110) planes.

In our nanotower project, we prepare large numbers of small 'towers' by lithographic etching of multiple bilayer structures on silicon wafers. In this way, well-defined metal faces can be prepared, and sufficient surface area is available to perform catalysis. These highly ordered arrays of nanotowers are important as model catalysts for metal-catalyzed reactions as well as for trying out the manufacture of future generations of catalyst. These new catalysts will have to be far more sophisticated than the present generation and, thus, require more sophisticated methods of manufacture.

Intercalated Sulfides

Crystalline, amorphous, and intercalation compounds of MoS_2 show a variety of unusual structural, electronic, and optical properties. They are used as solid-state lubricants, as catalysts in hydrotreating reactions (crystalline and amorphous MoS_2-type compounds, respectively), and as cathode material in alkali-metal batteries (MoS_3). A review concerning the chemical and catalytic properties of transition-metal sulfides has been published recently [1].

Intercalation compounds of molybdenum disulfide with a non-stoichiometric number of atoms, ions, or molecules, located between the layers of MoS_2 (M_xMoS_2-type compounds, $x \leq 1$), are of increasing importance for fundamental and applied research. Depending on the kind of species intercalated between the MoS_2 layers, materials with a variety of unusual properties can be prepared, *e.g.*, the so-called nanocomposites where organic macromolecules are located between the MoS_2 layers. Intercalation compounds also provide useful solid-state models for different types of bioinorganic systems and heterogeneous catalysts, such as the nitrogenase cofactor (M = Fe-porphyrine), hydrotreating catalysts ($M = Co^{2+}$, Ni^{2+}), or catalysts for the water-gas-shift reaction ($M = Na^+$, K^+). Whereas Fe or Cu are industrially used as catalysts in the water-gas-shift reaction ($CO + H_2O \rightarrow CO_2 + H_2$), MoS_2-type phases promoted by potassium have been recently recognized as alternative catalytically active material. Here, the activation of H_2O molecules on the potassium-promoted MoS_2 surface is of particular interest and can be studied conveniently using the hydrated intercalation compound $K_x(H_2O)_yMoS_2$ as a model catalyst.

A common property of the above-mentioned Mo-S compounds is their behavior during thermal treatment, *i.e.*, they are converted to the thermodynamically stable 2H-MoS_2. 2H-MoS_2 is a semiconductor and consists of stacks of slabs, each of which is composed of two layers of sulfur atoms with a layer of molybdenum atoms between them. Every Mo center is coordinated to six sulfur ligands in a regular trigonal prismatic arrangement. The interaction between two neighboring MoS_2 slabs is rather weak and corresponds to *van der Waals* forces [2]. Whereas 2H-MoS_2 has been known for a long time, the metastable 1T modification was discovered only a few years ago while investigating the above-mentioned intercalation compounds. 1T-MoS_2 has a distorted CdI_2-type structure and shows metallic behavior [3]. In the crystalline state, all Mo centers are coordinated to six sulfur ligands in a distorted octahedral arrangement. A schematic presentation of the bulk structures of 2H- and 1T-MoS_2 and of the intercalation compound $K_x(H_2O)_y$-MoS_2 can be found in the upper part of *Fig. 1*.

2H-MoS_2 can quite easily be prepared by heating stoichiometric amounts of the elements in inert gas or by heating MoO_3-type phases in H_2/H_2S atmospheres. 1T-MoS_2 is usually prepared by oxidation of $K_x(H_2O)_yMoS_2$ with I_2/CH_3CN, whereas $K_x(H_2O)_yMoS_2$ can be obtained from K_2MoO_4 by sulfidation ($K_2MoO_4 + 4\,H_2S$

**Correspondence*: Prof. Dr. R. Prins
Laboratory for Technical Chemistry
ETH-Zentrum
Universitätstrasse 6
CH–8092 Zürich
Tel.: + 41 1 632 54 90, Fax: + 41 1 632 11 62
E-Mail: prins@tech.chem.ethz.ch

CHIMIA 52 (1998) Nr. 10 (Oktober)

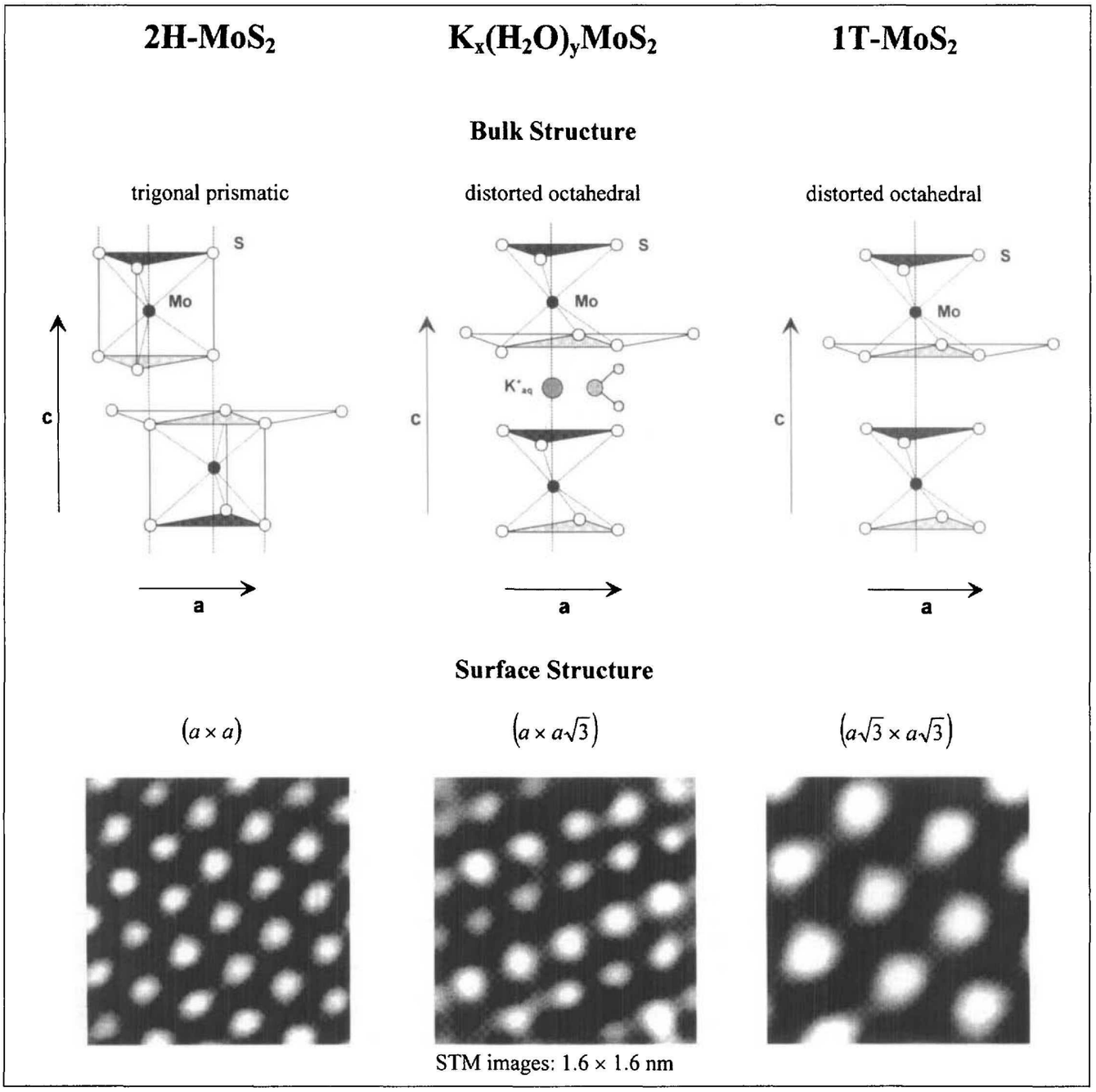

Fig. 1. *Bulk and surface structures of 2H-MoS_2, $K_x(H_2O)_yMoS_2$, and 1T-MoS_2.* The STM images were obtained with negative bias voltages and represent a sample region of 1.6 × 1.6 nm.

→ K_2MoS_4 + 4 H_2O), subsequent reduction (2 K_2MoS_4 + 3 H_2 → 2 K_zMoS_2 + 2y K^0 + K_2S + 3 H_2S, $y < 1$, $z = 1 - y$) and hydration (K_zMoS_2 + (n + y) H_2O → $K_x(H_2O)_yMoS_2$ + n/2 H_2 + n KOH, $x = z - n$). A detailed description of the synthesis can be found in [4].

Due to the presence of the intercalated K^+ cations, significant structural changes of the underlying MoS_2 structure emerge. The major reason lies in a change in the local coordination geometry of molybdenum from trigonal prismatic (as in the stable 2H-MoS_2) to distorted octahedral (as in the metastable 1T-MoS_2). The intercalation of cationic species between the layers of 2H-MoS_2 can, therefore, be considered to be a 2H → 1T phase transition. The change in the coordination geometry of molybdenum goes along with the formation of different types of superstructures, which can be characterized nicely by means of scanning tunnelling microscopy (STM), as shown in the lower part of *Fig. 1*. In $K_x(H_2O)_yMoS_2$ ($x \approx 0.3$), hydrated K^+ cations are located between the MoS_2 layers. Due to distortions within the crystallographic (a,b) plane, rows of sulfur atoms form along the b-axis [4] and lead to a monoclinic structure ($a \times a\sqrt{3}$ superstructure), as in the case of WTe_2. In 1T-MoS_2, the Mo centers are displaced from their ideal positions, so that three

Mo centers always come closer to each other (trimerization) and an $a\sqrt{3} \times a\sqrt{3}$ superstructure forms (a: lattice parameter of 2H-MoS_2 = 316 pm). The structural evolution in this series of compounds can be described by the following types of superstructures: 2H-MoS_2 ($a \times a$) → K_zMoS_2 ($2a \times 2a$) → $K_x(H_2O)_yMoS_2$ ($a \times a\sqrt{3}$) → 1T-MoS_2 ($a\sqrt{3} \times a\sqrt{3}$) [5].

CHIMIA 52 (1998) Nr. 10 (Oktober)

Mesoporous and Microporous Solids for Catalytic Applications

Heterogeneous catalysts offer significant advantages over their homogeneous counterparts, such as ease of separation, regenerability, and reusability. They are ideally suited for continuous flow-through operation in a fixed or fluidized bed. This is highly desirable in industrial applications, from an economical point of view. Zeolites have attracted wide interest as heterogeneous catalysts and adsorbents. They exhibit a high degree of uniform acidity, excellent thermal stability, and the potential for introducing shape selectivity due to the confined space inside their pores and the narrowness of the pores, in the order of 0.3–0.7 nm. Despite the benefits that may arise from exploiting shape selectivity, the microporous nature of zeolites can also be a serious drawback. Bulky molecules may be prevented from penetrating the pore system or may be subject to serious mass transport limitation which hinders their removal from the zeolite. In order to avoid these disadvantages while preserving the shape-selective properties, the creation of a secondary pore system with significantly larger pore diameters is desirable. This would enable a rapid transport of reactants and products to and from the shape-selective reaction centers.

Dealumination, the controlled removal of aluminium from the zeolite framework by hydrothermal treatment or by leaching with acids, is one way of generating such mesopores. The zeolite materials, obtained after various dealumination treatments, differ substantially with respect to their physical-chemical and catalytic properties. A detailed and comprehensive research program is in progress in our group. Its aim is to understand the mechanism of dealumination and to correlate the physical-chemical properties of post-synthesis modified zeolitic materials with their performance as catalysts and adsorbents.

A combined treatment of deep-bed calcination and subsequent acid leaching was found to be very effective for the formation of a secondary pore system containing mesopores. *Fig. 2* shows the SiO_2/Al_2O_3 ratio of H-mordenite calcined at 750° and dependent on the duration of acid treatment. The higher ratio obtained after using oxalic acid demonstrates that this acid is more efficient than nitric acid in removing aluminium from the zeolite because of the chelating nature of the oxalate anion. Nitric-acid leaching leads to the formation of meso- and macropores. Nitric acid dissolves a part of the silica framework of the zeolite, thereby carving a secondary pore system into the zeolite matrix. The roughening of the zeolite crystal surface, as expected to result form such a treatment, is clearly observable in the SEM pictures in *Fig. 3*. The crystallinity was retained in both cases, as confirmed

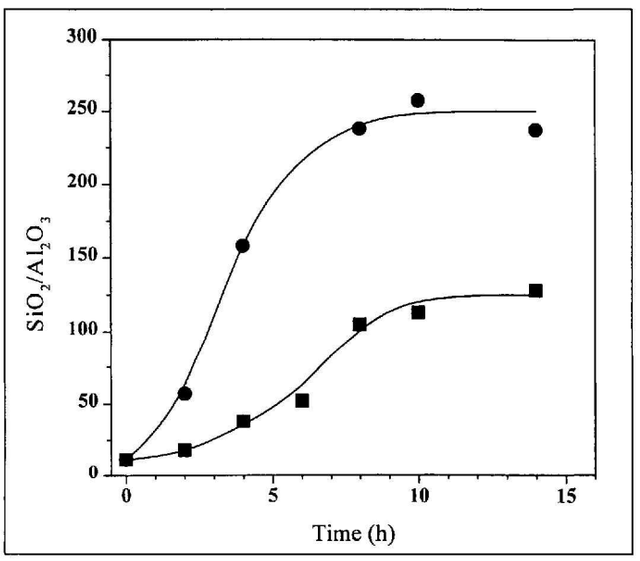

Fig. 2. *Dependence of the SiO_2/Al_2O_3 ratio of H-mordenite on dealumination with (●) 2M oxalic acid or (■) 2M nitric acid at reflux temperature and for various times*

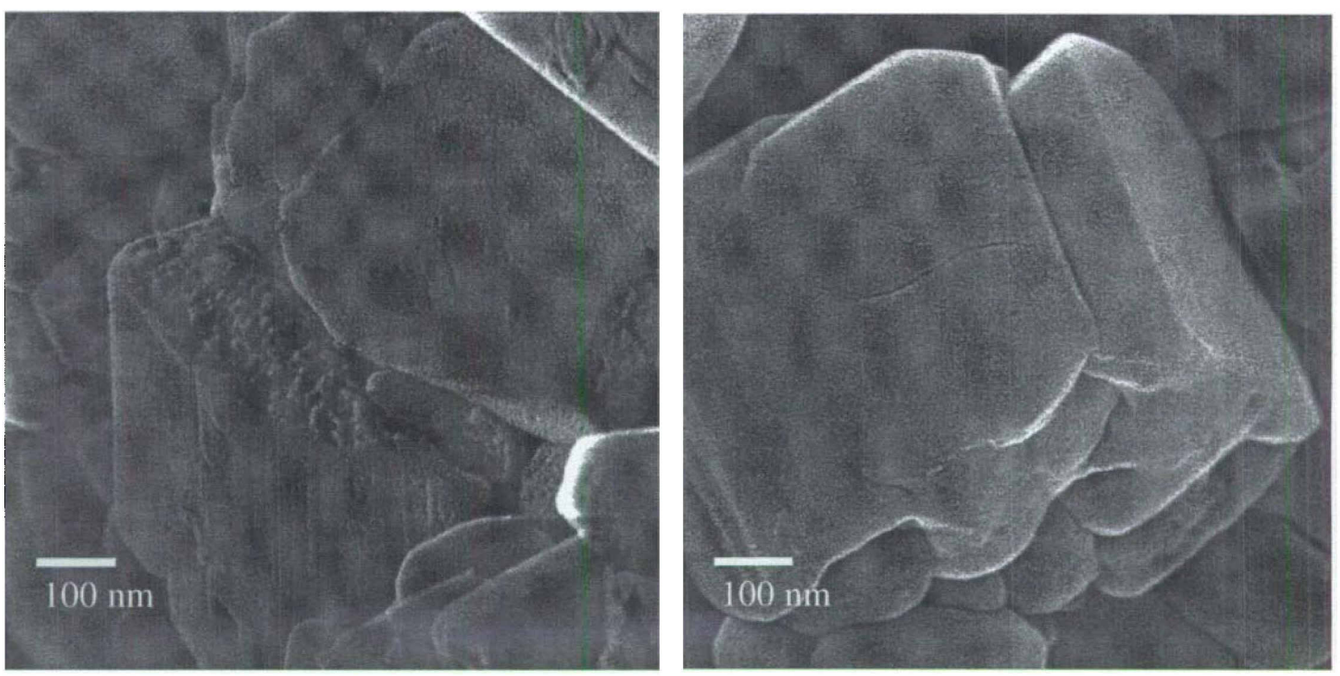

Fig. 3. *Surface roughening of H-mordenite after acid treatment as depicted by SEM; nitric acid* (left) *oxalic acid* (right)

CHIMIA 52 (1998) Nr. 10 (Oktober)

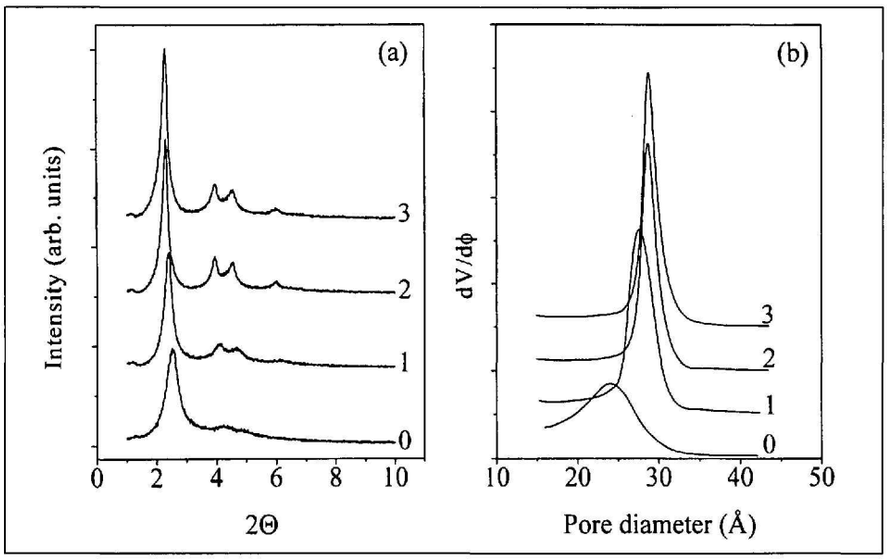

Fig. 4. a) *Powder XRD patterns and* b) *pore-size distribution of Al-MCM-41 that was synthesized with the indicated number of pH adjustments*

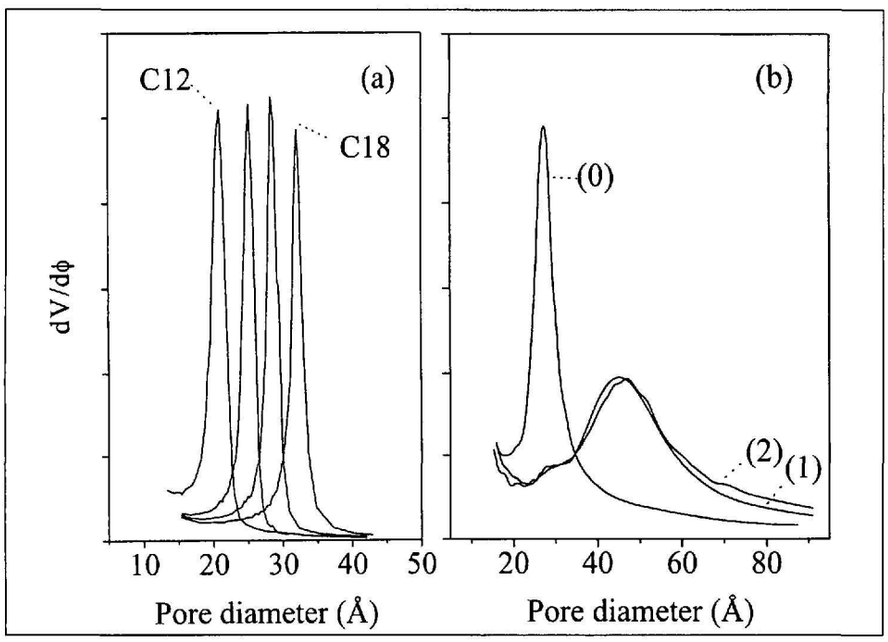

Fig. 5. *Dependence of the pore diameter of MCM-41* a) *on the surfactant hydrocarbon chain length and* b) *on increasing amounts of dodecane used as swelling agent* (molar dodecane-to-silica ratio is indicated)

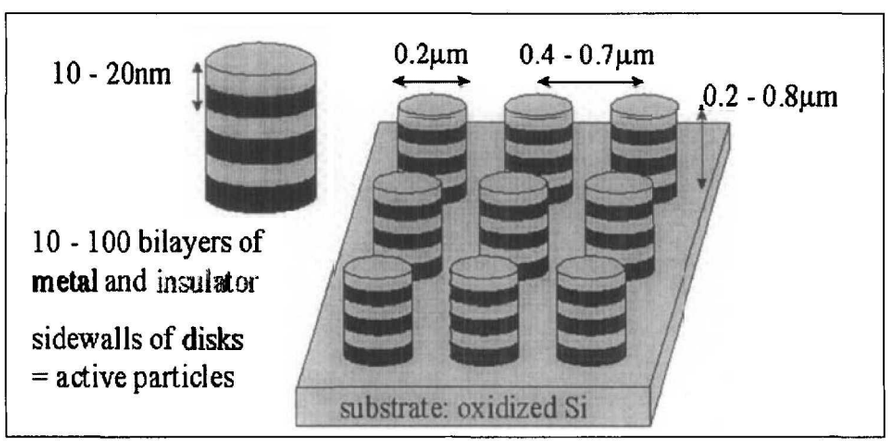

Fig. 6. *Scheme of nanotower system*

by powder XRD patterns of the zeolites before and after dealumination. An improvement in the catalytic performance of such zeolites has been demonstrated by a previous study in which mordenite, treated with nitric acid, exhibited enhanced long-term stability during the vapor-phase nitration of benzene [6].

The creation of a secondary pore system is insufficient, however, when molecules are too big to fit into the microporous channel system of zeolites. This concern has grown with the increasing application of zeolites to fine chemicals and the synthesis of intermediates where bulky molecules are usually the substrates of particular interest. Zeolites with larger pore dimensions have been rarely synthesized and have exhibited only limited stability toward dehydration and treatment at elevated temperatures. The discovery of MCM-type materials led to the belief that a mesoporous zeolitic material was finally within reach [7]. MCM-41, the hexagonal form of ordered, mesoporous molecular sieves is synthesized hydrothermally using surfactant micelles as the templating agent. Due to the amorphous structure of the MCM-41 walls, aluminium incorporated into the MCM-41 structure does not become as acid as the zeolites. The well-defined pore diameter together with a narrow pore-size distribution make MCM-41 the material of choice for mesoporous molecular sieves.

The structural quality of MCM-41 materials can be improved by adjusting the pH of the synthesis mixture. The better resolution and the presence of higher-order reflections in the powder XRD patterns of Al-MCM-41, obtained after the intermediate adjustment of the pH of the synthesis mixture to 11 in 24 h intervals, indicates an increase in the long-range order of Al-MCM-41 (*Fig. 4, a*). The increased order is paralleled by a narrower pore-size distribution, exemplified by an analysis of N_2 adsorption (*Fig. 4, b*). These effects led to an almost two-fold increase in the catalytic activity of the acylation of 2-methoxynaphthalene by acetic anhydride.

The pore diameter of MCM-41 depends on the size of the micelle used for templating. The size can be influenced easily by adjusting the length of the *n*-alkyl moiety of the alkyltrimethylammonium salt used as a surfactant molecule (*Fig. 5, a*). Unfortunately, C_{18} represents the upper limit because of its limited aqueous solubility. Reports that swelling of the micelles with increasing amounts of mesitylene led to MCM-41 materials with pore diameters of up to 10 nm [7] could

CHIMIA 52 (1998) Nr. 10 (Oktober)

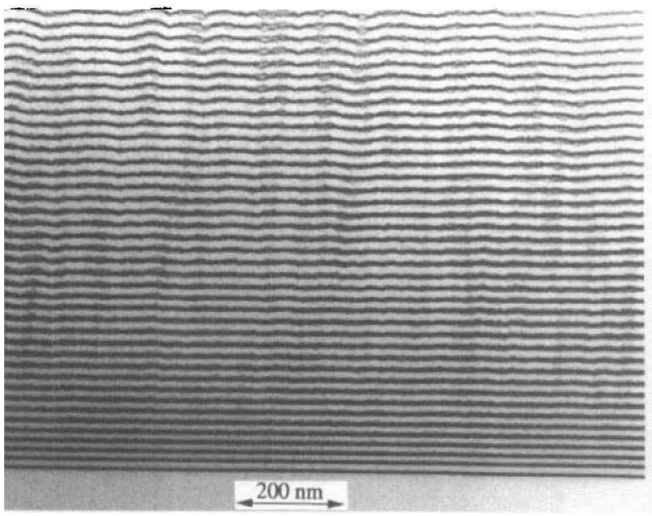

Fig. 7. *Transmission electron micrograph of 40 silica/Pd bilayers*

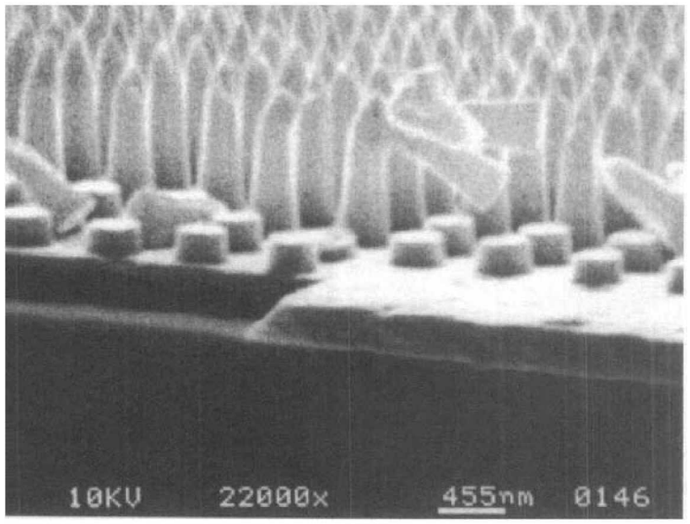

Fig. 8. *Scanning electron micrograph of partially etched nanotowers*

not be substantiated. Using dodecane as a swelling agent proved to be much more successful. *Fig. 5, b*, shows the pore-size distribution for pure silica MCM-41 that was synthesized using various amounts of dodecane for micelle enlargement. The result was MCM-41 with an average pore size of 5 nm. In a subsequent treatment, these materials will be modified by grafting alkyl- or phenyl-trimethoxy silane onto these surfaces with terminating mercapto, amino, or other functional groups, thereby allowing the generation of solid catalysts with a high density of acidic or basic sites. Due to their geometric arrangement, these catalysts make ideal supports for the immobilization of expensive catalytic materials, as was recently demonstrated [8].

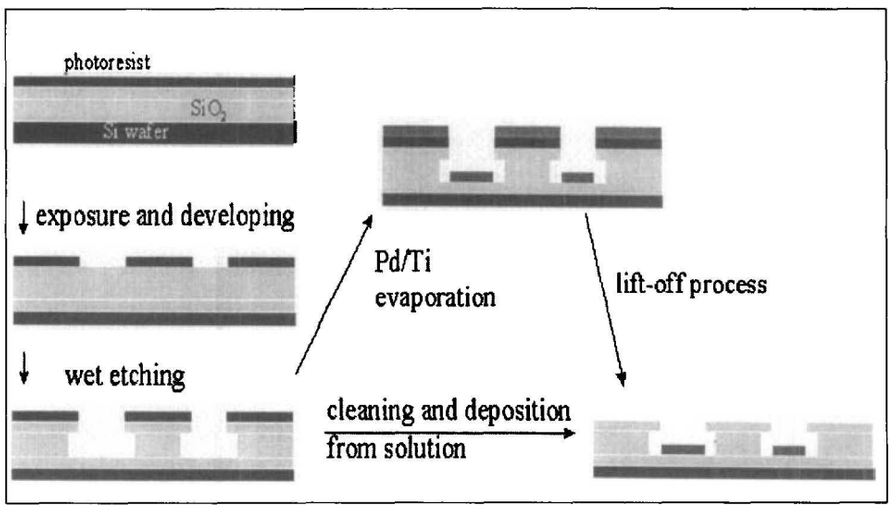

Fig. 9. *Scheme of 'hole sample' process*

Nanostructured Systems as Heterogeneous Model Catalysts

To achieve more insight into heterogeneous catalytic reactions, we present new ways of building and testing model catalysts by means of nanotechnology, especially nanolithography. Numerous attempts have been made to produce highly defined metal-particle arrays on flat substrates (*e.g.*, oxidized single-crystal surfaces) by electron-beam lithography [9–11]. However, these well-ordered systems can only be produced on very small areas (usually a few square micrometers) and are not stable under reactive conditions (oxidizing gas atmospheres at higher temperatures). Furthermore, their manufacture is very time-consuming. Our goal is to build systems that offer comparable homogeneity in the size and structure of the catalytically active species and that they can be produced faster and are stable under catalytic reactions. With our method, nanometer-sized structures can be produced over the surface of a 10-cm wafer in a few minutes.

First, we use oxidized silicon wafers supporting stacks of palladium and silica disks in a well-ordered array (*Fig. 6*). The catalytically active particles in this system are the perimeters of the metal disks. Their thickness can be varied from *ca.* 2–10 nm. The diameter of the towers is in the range of 200 nm, the array periodicity *ca.* 700 nm. One cm^2 of the silicon wafer contains *ca.* $2 \cdot 10^8$ nanotowers. Four Pd/silica layers, made by sputter deposition onto the oxidized silicon wafer, are now available (*Fig. 7*). Therefore, 1 cm^2 of a structured wafer contains $8 \cdot 10^9$ Pd disks of equal size with a total active area of *ca.* 0.3 cm^2.

The lateral structure is made by exposing a three-layer-photoresistant material on top of the bilayers to an interference pattern of broadened laser beams. In this way, a whole 10-cm wafer can be homogeneously patterned in a few minutes. The multilayers are subsequently structured by ion milling through the existing photoresist grid.

Fig. 8 shows an electron micrograph of a cleaved wafer, that has not been fully etched in the ion-milling machine and is not yet completely free of resist residues. There is oxidized silicon from the top to the bottom of the wafer, of the unetched part of the silica/Pd multilayer, of the etched part (forming small towers), and of finger-like columns of resist. The tops of the latter are conical due to being etched by the ion-milling process.

A second system, that has already been used for preliminary tests of stability and catalytic properties, is the so-called 'hole sample'. It is made according to the same manufacturing scheme as the nanotowers (*Fig. 9*). Double exposure of photoresistant material spun on a very thick SiO_2 layer (*ca.* 150 nm) leads to an etching mask. Wet-chemical etching then leads to shallow holes in the oxide substrate (*Fig.*

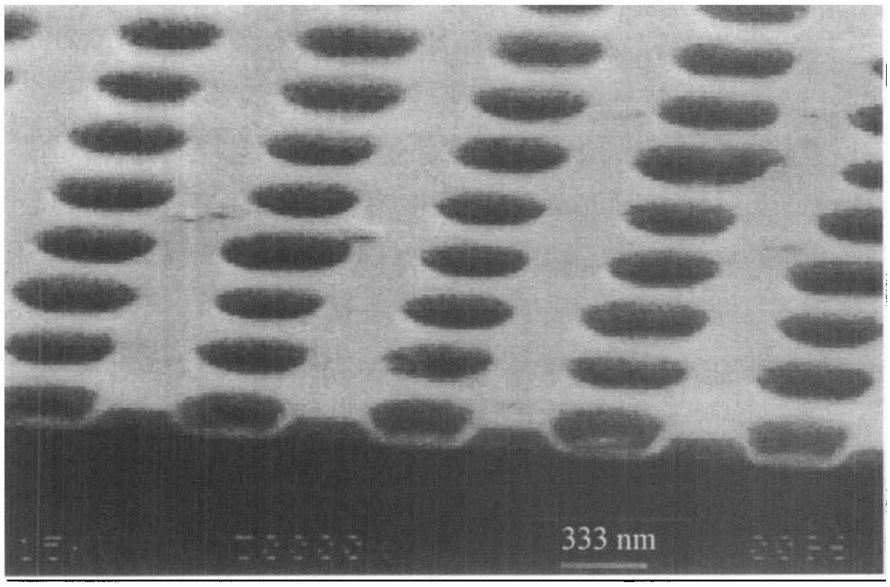

Fig. 10. *Scanning electron micrograph of 'hole sample'*

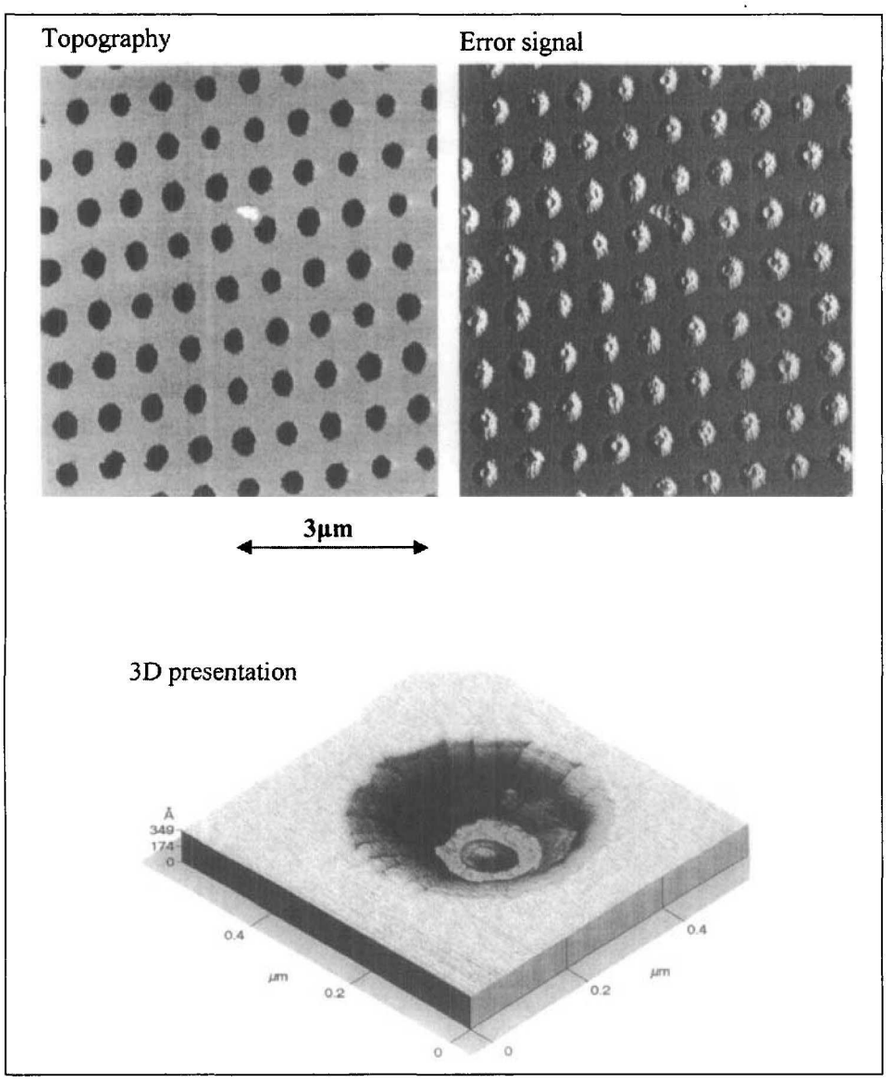

Fig. 11. *AFM pictures of a nanostructured SiO_2 surface loaded with copper clusters.* Deposition was done by spin coating a 1 wt.-% solution of $Cu(NO_3)_2$ in butan-1-ol. The sample was thereafter annealed in UHV and reduced. The holes have diameters of *ca.* 300 nm and are 50–70 nm in depth. Because of the limited grey scale values, the particles (heights 10 nm, diameters < 100 nm) are only visible in error signal and 3D presentation.

10). These samples are used as substrates for the deposition of metal as the active material. By evaporating metal or deposition from metal-salt solution, clusters can be formed which reside in these holes. The first method is sketched in *Fig. 9*. A thin metal film is evaporated on the structured samples before removing the resist. After the liftoff process, only the bottoms of the holes are covered by metal. After subsequent heating in oxidizing and reducing atmospheres, the films can be reconstructed to localized spherical particles. A second possibility is more comparable to wet-chemical catalyst impregnation. Hereby, metal-salt solutions are spincoated onto the structured surfaces. Calcination (heating in air) and reduction/oxidation cycles lead to metal particles. Under the appropriate conditions, we can locate the particles right at the bottom of the holes, as shown in *Fig. 11*.

First tests have shown that these systems are stable up to 500°, and that they can be used and investigated under ultra high vacuum (UHV) conditions as well as under atmospheric pressures. With these materials we will be able to bridge the pressure and material gaps between model and industrial catalysts.

Received: July 3, 1998

[1] 'Transition Metal Sulphides – Chemistry and Catalysis', Eds. T. Weber, R. Prins, and R.A. van Santen, Kluwer Academic Publishers, Drodrecht, 1998.
[2] R.G. Dickinson, L. Pauling, *J. Am. Chem. Soc.* **1923**, *45*, 1466; K.D. Bronsema, J.L. de Boer, F. Jellinek, *Z. Anorg. Allg. Chem.* **1986**, *540/541*, 15.
[3] F. Wypych, R. Schöllhorn, *J. Chem. Soc., Chem. Commun.* **1992**, 1386.
[4] F. Wypych, T. Weber, R. Prins, *Surf. Sci.* **1997**, *380*, L474.
[5] F. Wypych, T. Weber, R. Prins, *Chem. Mater.* **1998**, *10*, 723.
[6] L. Bertea, H.W. Kouwenhoven, R. Prins, *Appl. Catal., A: General* **1995**, *129*, 229.
[7] J.S. Beck, J.C. Vartuli, W.J. Roth, M.E. Leonowicz, C.T. Kresge, K.D. Schmitt, C.T.-W. Chu, D.H. Olson, E.W. Sheppard, S.B. McCullen, J.B. Higgins, J.L. Schlenker, *J. Am. Chem. Soc.* **1992**, *114*, 10834; C.T. Kresge, M.E. Leonowicz, W.J. Roth, J.C. Vartuli, J.S. Beck, *Nature (London)* **1992**, *359*, 710.
[8] S. Krijnen, H.C.L. Abbenhuis, R.W.J.M. Hanssen, J.H.C. van Hooff, R.A. van Santen, *Angew. Chem., Int. Ed. Engl.* **1998**, *37*, 356.
[9] M.X. Yang, D.H. Gracias, P.W. Jacobs, G.A. Somorjai, *Langmuir* **1998**, *14(6)*, 1458.
[10] M.X. Yang, P.W. Jacobs, C. Yoon, L. Muray, E. Anderson, D. Attwood, G.A. Somorjai, *Catal. Lett.* **1998**, *45*, 5.
[11] A.C. Krauth, K.H. Lee, G.H. Bernstein, E.E. Wolf, *Catal. Lett.* **1994**, *27*, 43.